



Title	Deep mantle roots and continental emergence: implications for whole-Earth elemental cycling, long-term climate, and the Cambrian explosion
Author(s)	Lee, CT; Caves, J; Jiang, J; Cao, W; Lenardic, A; Mc Kenzie, NR; Shorttle, O; Yin, QZ; Dyer, B
Citation	International Geology Review, 2017, v. 60 n. 4, p. 431-448
Issued Date	2017
URL	http://hdl.handle.net/10722/247361
Rights	This work is licensed under a Creative Commons Attribution-NonCommercial-NoDerivatives 4.0 International License.

ARTICLE



Deep mantle roots and continental emergence: implications for whole-Earth elemental cycling, long-term climate, and the Cambrian explosion

Cin-Ty A. Lee^a, Jeremy Caves^b, Hehe Jiang^a, Wenrong Cao^{a,c}, Adrian Lenardic^a, N. Ryan McKenzie^d, Oliver Shorttle^e, Qing-zhu Yin^f and Blake Dyer^g

^aDepartment of Earth, Environmental and Planetary Sciences, Rice University, Houston, TX, USA; ^bDepartment of Earth Sciences, ETH Zürich, Zürich, Switzerland; ^cDepartment of Geological Sciences and Engineering, University of Nevada, Reno, CA, USA; ^dDepartment of Earth Sciences, University of Hong Kong, Hong Kong, China; ^eDepartment of Earth Sciences, University of Cambridge, Cambridge, UK; ^fDepartment of Earth and Planetary Sciences, University of California, Davis, CA, USA; ^gLamont-Doherty Earth Observatory, Columbia University, Palisades, NY, USA

ABSTRACT

Elevations on Earth are dominantly controlled by crustal buoyancy, primarily through variations in crustal thickness: continents ride higher than ocean basins because they are underlain by thicker crust. Mountain building, where crust is magmatically or tectonically thickened, is thus key to making continents. However, most of the continents have long passed their mountain building origins, having since subsided back to near sea level. The elevations of the old, stable continents are lower than that expected for their crustal thicknesses, requiring a subcrustal component of negative buoyancy that develops after mountain building. While initial subsidence is driven by crustal erosion, thermal relaxation through growth of a cold thermal boundary layer provides the negative buoyancy that causes continents to subside further. The maximum thickness of this thermal boundary layer is controlled by the thickness of a chemically and rheologically distinct continental mantle root, formed during large-scale mantle melting billions of years ago. The final resting elevation of a stabilized continent is controlled by the thickness of this thermal boundary layer and the temperature of the Earth's mantle, such that continents ride higher in a cooler mantle and lower in a hot mantle. Constrained by the thermal history of the Earth, continents are predicted to have been mostly below sea level for most of Earth's history, with areas of land being confined to narrow strips of active mountain building. Large-scale emergence of stable continents occurred late in Earth's history (Neoproterozoic) over a 100–300 million year transition, irreversibly altering the surface of the Earth in terms of weathering, climate, biogeochemical cycling and the evolution of life. Climate during the transition would be expected to be unstable, swinging back and forth between icehouse and greenhouse states as higher order fluctuations in mantle dynamics would cause the Earth to fluctuate rapidly between water and terrestrial worlds.

ARTICLE HISTORY

Received 4 June 2017
Accepted 7 June 2017

KEYWORDS



Earth history; climate; continents; lithosphere; elevation; crust; unconformity; peridotite

Introduction

The Earth has a bimodal hypsometry (Figure 1(a)). Continents, bounded by the edge of the continental shelf, ride 3–4 km above ocean basins. For the most part, continents ride near or just above sea level and are characterized by low relief. These regions of low relief tend to be the old, stabilized portions of continents. Some fraction of the continents is represented by shallowly submerged continental shelves. Unusually high elevations are limited to mountain belts characterized by active tectonism or magmatism.

It is widely agreed that orogenic processes, through convergent tectonics or magmatism, are critical to the formation of continental crust, unlike oceanic crust, which is formed by magmatism in divergent spreading centres. That

is, mountain building, as exemplified by the modern Andes and Tibet, plays a key role in the birth of a continent. Although most parts of the continents are old, stabilized, and of low relief, vestiges of an orogenic birth are seen in the deeply exhumed igneous or metamorphosed basement rocks. Of interest here is how the elevations of continental crust evolve through time, from the high elevations of active crust formation to the low elevations characterizing stabilized continents today. Thick packages of Proterozoic to Palaeozoic sedimentary sequences draped across vast areas of the continents and time-correlative over multiple continents suggest that stabilized continents were globally below sea level for long time intervals, forming large expanses of shallow epi-continental seas (Sloss 1963; Eriksson *et al.* 2006). The sediments themselves overlie deeply exhumed igneous or metamorphic basement of

CONTACT Cin-Ty A. Lee  ctlee@rice.edu  Department of Earth, Environmental and Planetary Sciences, Rice University, Houston, TX, USA

© 2017 The Author(s). Published by Informa UK Limited, trading as Taylor & Francis Group.

This is an Open Access article distributed under the terms of the Creative Commons Attribution-NonCommercial-NoDerivatives License (<http://creativecommons.org/licenses/by-nc-nd/4.0/>), which permits non-commercial re-use, distribution, and reproduction in any medium, provided the original work is properly cited, and is not altered, transformed, or built upon in any way.

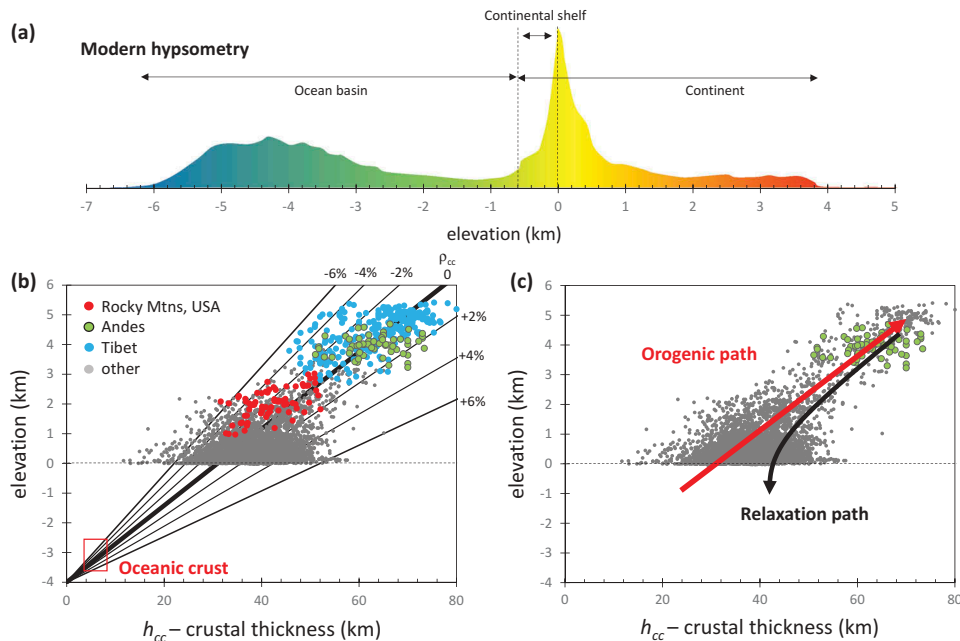


Figure 1. (a) Modern hypsometry. Continents include the submerged continental shelf. Vertical axis represents proportional area. (b) Elevation versus crustal thickness from Crust 1.0 (Laske *et al.* 2013). Mountain array indicates elevations largely controlled by crustal thickness. Sloped lines correspond to effective crustal densities in terms of percentage variation from a reference crustal density of 2.9 g/cm^3 (Hasterock and Chapman 2007) and a mantle compositional density of 3.35 g/cm^3 (Lee *et al.* 2015). Average elevation of mid-oceanic ridges and oceanic crust is also shown. No reasonable crustal densities can explain the low elevations of stable continental interiors (Cratons). (c) Mountain building is defined by the orogenic path and involves coupled crustal thickening and erosion. Stable continental interiors must follow a relaxation path deviating from the orogenic trend. This relaxation path requires both crustal erosion and growth of a thermal boundary layer.

middle Proterozoic to Archaean age, typically with hundreds of millions of years missing between the basement and the oldest sediment (Peters and Gaines 2012). These deeply exhumed basement rocks are often minimally retrogressed, consistent with continents initially undergoing a rapid erosional phase during their orogenic beginnings. The ensuing gap in the geologic record, followed by long periods of sediment accumulation, indicates that after orogenic forcing wanes, continents subside.

Key questions that arise are as follows. How fast do mountain belts subside and what processes control subsidence? What dictates the terminal resting elevation of stabilized continents? Do mountain belts eventually submerge below sea level? Is the present day emergent state of continents representative of Earth's history, or if emergence is anomalous, when did continents as a whole emerge above sea level? How the elevations of mountains and stabilized continents evolved through Earth's history is critical to understanding whether the Earth has undergone fundamental changes in albedo, ocean circulation, hydrology, weathering, sediment formation and deposition, and biogeochemical cycling. The objective of this paper is thus to explore the elevational history of a continent, from birth to stabilization.

The elevational history of a continent

On long timescales ($>10 \text{ ky}$) and wavelengths ($>10\text{--}100 \text{ km}$), continents, ocean basins, and mountains have indistinguishable free-air gravity signatures, indicating that they are in isostatic equilibrium and that their elevations are largely controlled by buoyancy, with dynamic effects of secondary importance (Ewing and Press 1955; Phillips and Lambeck 1980; Wicczorek 2007). The observation that mountain elevation correlates with crustal thickness (Figure 1(b)) means that continents 'float' buoyantly on top of a 'fluid' mantle. Continents float, of course, because the density of crust is less than that of the mantle. However, *variations* in elevation are primarily controlled by crustal thickness, with mantle effects, dynamic topography and lateral variations in crustal density playing a secondary role (Hasterock and Chapman 2007). The effect of crustal thickness can be seen in Figure 1(b). Ocean basins ride 3–4 km below most continents because they are underlain by crust of 7–10 km thickness whereas the thickness of continental crust is generally 30 km or greater. It can also be seen that continental elevations correlate with crustal thickness. Although basaltic crust is denser than andesitic crust, the differences are small ($<6\%$; (Fliedner and Klempner 2000; Brocher 2005))

compared to the effect of variations in crustal thickness. The exact relationship between elevation h_e and crustal thickness h_{cc} in mountain belts is controlled by the average effective density contrast between the crust ρ_{cc} and the ambient convecting mantle ρ_a , that is, the rise of a mountain follows a well-defined 'orogenic path', whose slope in terms of elevation versus crustal thickness is defined by the *effective* density contrast between the crust and the mantle, $dh_e/dh_{cc} = 1 - \rho_{cc}/\rho_a$ (Figure 1(b)) (Hasterock and Chapman 2007; Lee *et al.* 2015). Crustal thickness-elevation slopes, pinned to the mid-ocean ridge, are shown in Figure 1(b) assuming a continental crustal density of 2.9 g/cm^3 and a mantle density of 3.35 g/cm^3 (Hasterock and Chapman 2007).

Although crustal thickness can explain variations in elevation in active mountain belts, it is curious that the low relief, tectonically stable interiors of continents fall below the orogenic path (Figure 1(b,c)), too low for their crustal thicknesses (Hasterock and Chapman 2007). A similar observation was noted by Fischer (2002), who referred to this phenomenon as a 'waning buoyancy' of an aging mountain belt. Typical crustal densities required to explain these low elevations are unreasonably high (Figure 1(b)). Fischer suggested that cooling of the orogenic belt might lead to eclogitization of the lowermost crust, giving rise to a compositional densification that would explain the anomalously low elevations of stabilized continents. However, eclogite xenoliths are generally rare in most

xenolith-bearing volcanics that traverse continental lithosphere. Another possibility is the presence of ancient eclogite lenses within ancient continental lithosphere itself (Kelly *et al.* 2003), but again, such lithologies may not be pervasive. Furthermore, when present, such lithologies appear to be as old as the continental crust itself and, therefore, cannot explain a 'waning' buoyancy.

Here, we explore the possibility that the anomalously low elevations of continents is due to a growing contribution of negative thermal buoyancy below the crust as mountain belts age. This negative thermal buoyancy is represented by the mantle part of the cold thermal boundary (corresponding roughly with the lithosphere) underlying the stable continents. Due to thermal contraction, the thermal boundary layer is denser than the ambient convecting mantle, causing subsidence, much like old ocean basins, which are also underlain by a cold boundary layer (Parsons and Sclater 1977; McKenzie and Priestley 2016) (Figure 2(a)). Thus, elevations of stable continental interiors, like ocean basins, must be modulated by the thickness h_{cr} and density ρ_{cr} of the underlying cold mantle root. This concept can be illustrated with a simplified isostatic relationship: $h_e = h_{cc}(1 - \rho_{cc}/\rho_a) + h_{cr}(1 - \rho_{cr}/\rho_a)$, where $\rho_{cr} > \rho_a$. The density of the mantle root relative to the ambient mantle is controlled by its intrinsic compositional density ρ_{cr}^0 and temperature relative to the ambient mantle. Approximating the continental geotherm as linear and assuming a constant temperature for the convecting

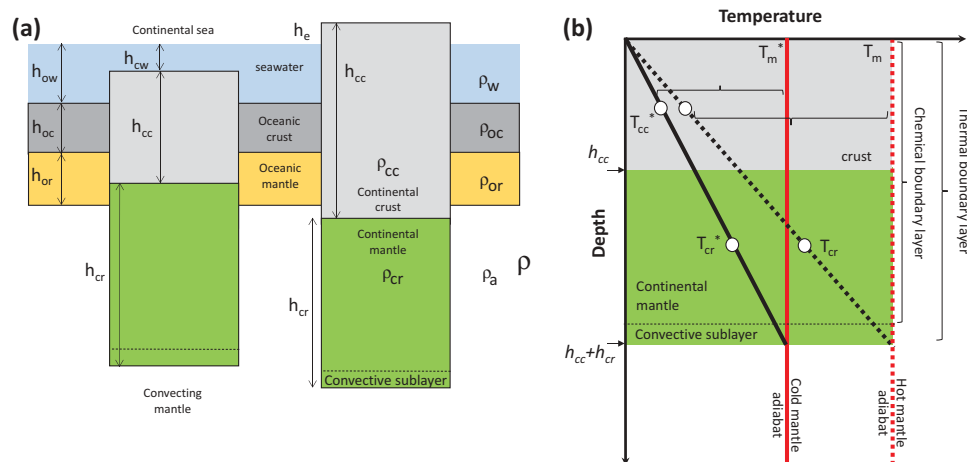


Figure 2. (a). Isostatic density columns for submerged and emergent continents (h_{ow} = oceanic water depth, h_{cw} = water depth above submerged continent, h_e = elevation above sea level for emergent continent, h_{oc} = oceanic crust thickness, h_{or} = oceanic mantle root thickness (lithospheric mantle), h_{cc} = continental crust thickness, h_{cr} = continental mantle root thickness, and ρ_w , ρ_{oc} , ρ_{or} , ρ_{cc} , ρ_{cr} , and ρ_a are densities of water, oceanic crust, oceanic mantle root, continental crust, continental mantle root, and asthenospheric mantle). (b). Chemical boundary layer represents depleted mantle root. Because it is rigid, it defines the thermal boundary layer thickness; a thin convective sublayer makes up the very base of the thermal boundary layer, just beneath the chemical boundary layer. The total thickness of the continental thermal boundary layer is $h_{cc} + h_{cr}$. Average temperatures of continental crust T_{cc} and continental mantle root T_{cr} , assuming thermal boundary layer can be approximated by a linear geotherm, basal temperature is equal to mantle potential temperature (temperature of asthenosphere T_m), and surface temperature is 0°C . Model allows for changes in thermal boundary layer thickness as well changes in mantle temperature (* corresponds to present day). Diagonal dashed and solid lines correspond to approximate geotherms for two different mantle potential temperatures T_m .

mantle T_m , the average temperature difference between the mantle root and the convecting mantle is (following McKenzie 1978) (Figure 2(b)):

$$\Delta T_{cr} = T_{cr} - T_m = T_m \left(\frac{-h_{cr}}{2(h_{cc} + h_{cr})} \right), \quad (1)$$

where the surface temperature of the Earth is assumed to be 0°C and density is $\rho_{cr} = \rho_a^o(1 - \alpha\Delta T_{cr})$, α is the thermal expansion coefficient ($3 \times 10^{-5}/^\circ\text{C}$) and ρ_a^o is the intrinsic compositional density at standard temperature and pressure (see Table 1). Incorporating Equation (1) into an isostatic balance that considers the effects of temperature on density yields:

$$h_e = (h_{cc} + h_{cr}) - \frac{\rho_{cc}^o}{\rho_a^o} \left[h_{cc} + \alpha T_m \frac{h_{cc}(2h_{cr} + h_{cc})}{2(h_{cc} + h_{cr})} \right] - \frac{\rho_{cr}^o}{\rho_a^o} \left[h_{cr} + \alpha T_m \frac{h_{cr}^2}{2(h_{cc} + h_{cr})} \right], \quad (2)$$

where ρ_a^o is the density of ambient convecting mantle at T_m , ρ_{cr}^o/ρ_a^o is the relative compositional density contrast between the mantle root and convecting mantle, and ρ_{cc}^o/ρ_a^o is the intrinsic compositional density contrast between the crust and the convecting mantle. Equation (2) shows that continental elevations increase when continental crust thickness increases, intrinsic density of the continental lithospheric mantle root decreases, or mantle potential temperature decreases. More comprehensive equations, which include the effects of ocean volume, thickness of oceanic crust and oceanic mantle, are presented in the Appendix.

Xenolith thermobarometry and seismic studies indicate that the thickness of the thermal boundary layer beneath the stable parts of continents extends to depths of ~150 to ~200 km, which is much thicker than the maximum depth of the oceanic thermal

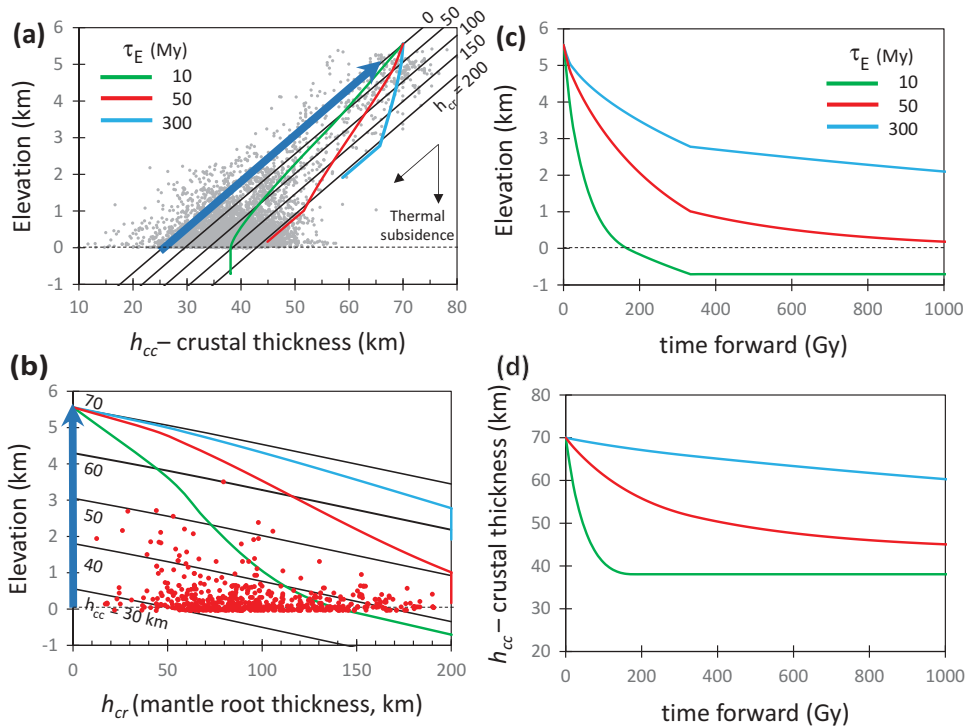


Figure 3. (a) Elevation (h_e) versus crustal thickness (h_{cc}), contoured (black diagonal lines) for different continental mantle root thicknesses (h_{cr}) following Equation (2). Thick, cold mantle roots decrease elevations. Crustal data from Figure 1(b) are shown. Thick blue arrow represents an orogenic path of crustal thickening and concomitant elevation rise. Thin green, red and blue lines represent relaxation paths corresponding to different erosional time constants (τ_E). Their slopes reflect relative differences between erosion (parallel to black diagonal contours) and thermal relaxation (vertical). In all relaxation calculations, thermal relaxation is terminated after $h_{cr} + h_{cc}$ equals 200 km (note that erosion may continue to operate if continent is still above sea level). All calculations assume mantle potential temperature is constant at 1350°C. (b) Same as in (a) but elevation is plotted against mantle root thickness, contoured (black straight lines) with crustal thickness (h_{cc}). Red circles represent mantle root thickness h_{cr} beneath cratons, which is the difference between the depth to the base of the thermal boundary layer and crustal thickness. Thermal boundary layer thicknesses are determined by extrapolation of surface heat flow to depth (Artemieva and Mooney 2001) and crustal thicknesses are determined by the depth to the Moho (Mooney *et al.* 1998). Coloured lines as in (a). (c) Relaxation paths showing decrease in elevation with time after all tectonic or magmatic forcings have ended. Coloured curves correspond to different erosional time constants and represent the same relaxation models as in (a) and (b). (d) Same relaxation paths as in (a–c), but showing crustal thickness as a function of time forward.

boundary layer (Jordan 1978; Gung *et al.* 2003; Lee *et al.* 2005, 2011; Pearson and Wittig 2008). For an average continental crustal thickness of 40 km, up to 75% of the thermal boundary layer is made up by the cold mantle root (h_{cr}) and the remaining ~25% by the crust. The peridotites that comprise the mantle root are depleted in Fe due to prior melt depletion during their formation (Jordan 1978, 1988); they are ~1% intrinsically less dense than the fertile ambient convecting mantle at the same temperature ($\rho_{cr}^o/\rho_a^o \sim 0.99$) (Lee 2003; Lee *et al.* 2011). This compositional density contrast, however, is not sufficient to completely counter-balance the effects of thermal contraction, perhaps manifested in the anomalously low elevations of stable continents. After factoring these compositional effects in, it can be seen from Figure 3(a) that the low elevations of stable continents can be explained by the presence of 50–150 km thick mantle roots. In active mountain belts, where the thermal boundary layer rarely exceeds 100 km in thickness, the crust dominates the thermal boundary layer and elevations plot on the ‘orogenic path’, controlled primarily by crustal thickness (Figure 3(a)). In Figure 3(b), we have also plotted independent constraints on mantle root thickness beneath cratons as determined from the difference between the depth to the base of the thermal boundary layer and Moho, the latter determined by extrapolation of surface heat flow-defined geotherms to depth (Artemieva and Mooney 2001) and the former from seismic crustal models (Mooney *et al.* 1998). These independent constraints on root thickness are consistent with our model predictions. We recognize that there are variations in thermal boundary layer thickness and continental mantle composition that will influence our calculations. Our goal here is not to dwell on these variations but rather to describe the first-order isostatic behaviour of continents.

The orogenic path

Making continents requires tectonic or magmatic thickening, but such thickening is modulated by erosion because erosion is controlled by elevation excess. The rate dh_{cc}/dt at which crustal thickness changes is balanced by the rate of magmatic or tectonic crustal thickening \dot{M} ($\text{km} \times \text{km}^{-2}$ million year $^{-1}$) minus the rate of erosion \dot{E} ($\text{km} \times \text{km}^{-2}$ million year $^{-1}$); that is, $dh_{cc}/dt = \dot{M} - \dot{E}$ (Lee *et al.* 2015). Isostasy requires that the rate of crustal thickening to be (Lee *et al.* 2015)

$$\frac{dh_{cc}}{dt} = \dot{M} - \frac{1}{\tau_E} \left(1 - \frac{\rho_{cc}}{\rho_a} \right) h_{cc}, \quad (3)$$

where $1/\tau_E$ represents a linear rate constant describing the efficiency of erosion and τ_E represents the characteristic response time for erosion, which depends on climate and substrate erodibility (Simoes *et al.* 2010). Typical erosional time constants (τ_E) are of the order of 5–10 million years, shorter than most orogenic intervals and thermal relaxation timescales (Lee *et al.* 2015). This implies that when mountains rise and initially subside, their elevations are controlled solely by crustal thickness and thus define the orogenic path $dh_e/dh_{cc} = (1 - \rho_{cc}/\rho_a)$ (Figure 1(b,c)). Furthermore, maximum erosion rates occur during crustal thickening because that is when elevations are highest. When crustal thickening processes stop, erosion rates decay rapidly as crustal thickness and elevation decrease. U–Th/He thermochronologic studies of cratons, for example, show that cratons underwent most of their erosion during their orogenic formative periods with subsequent minimal erosion (Flowers *et al.* 2006).

Subsidence along the relaxation path

After crustal thickening ends, mountains will decrease in elevation, initially by erosional thinning of the crust. However, after tens of millions of years, erosion rates decrease and thermal subsidence, through growth of a thermal boundary layer, becomes more important. Thermal boundary layers represent the uppermost part of convective systems through which vertical heat loss occurs by thermal diffusion and below which heat transfer occurs by advection. In the case of ocean basins, subsidence occurs as the seafloor moves away from the mid-ocean ridge due to growth of a thermal boundary layer and accompanying thermal contraction (Parsons and Sclater 1977). Eventually, the boundary layer grows to a critical thickness beyond which the oceanic boundary layer subducts back into the Earth. On Earth, the oceanic thermal boundary layer reaches a maximum thickness of ~100 km (Parsons and Sclater 1977; Parsons and McKenzie 1978) with the rate of thickening controlled by conductive cooling and thus scaling with the square root of time t , $R \sim \sqrt{4\kappa t}$, where κ is thermal diffusivity (10^{-6} m 2 /s).

Unlike ocean basins, the decay of a mountain belt involves both erosion and thermal relaxation. Timescales for eroding the crust should be <60 million years for $\tau_E \sim 5$ million years and 500 million years for $\tau_E \sim 100$ million years, the former typical of mountain belts where orographic precipitation is important and the latter more typical of stable continental interiors (Simoes *et al.* 2010). The timescales for thickening of a boundary layer to ~200 km takes ~500 million years. Because erosional timescales are shorter than thermal

relaxation timescales, elevation decrease follows a steeper trajectory in elevation (h_e) versus crustal thickness (h_{cc}) space (Figure 3(a–c)). When continental elevations decrease, erosion rates decrease, allowing thermal boundary layer thickening to catch up, thus resulting in subsidence without any further decrease in crustal thickness (Figure 3(d)). Continued growth of the thermal boundary layer will eventually cause continents to subside below sea-level, generating accommodation space for sediments (Figure 3(a–c)). Sedimentation can cause crustal thickness to increase again (within the limits defined by sea level). We have not accounted for deposition so the extents of subsidence below sea level calculated here are upper bounds. Our model shows that several hundred million years must pass between mountain building, when erosion peaks, and eventual submergence of a continent. This is how ‘great’ unconformities are made.

Continental mantle root thickness and terminal resting state

Based on xenolith and seismic studies, continental thermal boundary layers do not appear to exceed ~200 km (Gung *et al.* 2003), which exceeds the characteristic thermal thickness of the Earth as represented by oceanic thermal boundary layers (Cooper *et al.* 2004). However, unlike ocean basins, continents do not subduct, remaining stable and isolated from the convecting mantle since their formation (Pearson *et al.* 1995). Paradoxically, these thick continental thermal boundary layers should have foundered or thinned back to the characteristic thermal thickness of the convecting mantle. Continental thermal boundary layers must thus have unique properties that prevent them from thermally re-equilibrating with the convecting mantle. Although continental mantle is depleted in Fe from early melting events, making them intrinsically of low density (Jordan 1978), the anomalously low elevations of stable continents indicates that this positive chemical buoyancy is not sufficient alone to negate the negative thermal buoyancy (Figures 1(b) and 2). In addition to chemical buoyancy, the longevity of continental mantle is likely imparted by its intrinsic strength, which prevents it from being thermally thinned over time (Lenardic and Moresi 1999). Exactly why continental mantle is intrinsically strong is unclear, but it is generally thought that prior melt depletion events resulted in efficient removal of hydrogen, which increases viscosity (Pollack 1986; Hirth and Kohlstedt 1996). Whatever the cause, stable continents are thought to be underlain by thick and rigid chemical boundary layers, and it is the thickness of this immobile chemical boundary layer, a

long-lived property predefined from continent formation, which dictates and limits the thickness of the thermal boundary layer (Hirth *et al.* 2000; Lee *et al.* 2005; Cooper *et al.* 2006). Cooper *et al.* showed that when this rigid and hence non-convecting chemical boundary layer is thick, the convective sublayer beneath the chemical boundary layer is thin and the thickness of the thermal boundary layer is for all intents and purposes defined by the base of the chemical boundary layer. This chemical boundary layer, formed initially by melting, is thought to have subsequently thickened during the same orogenic events that gave rise to thick crust during the formation of the continent (Pearson and Wittig 2008; Lee and Chin 2014). Because the chemical boundary layer is formed by melting, it is initially hot so that the chemical boundary layer exceeds the thickness of the thermal boundary layer (which is only as thick as the crust during active orogeny). Only after thermal relaxation does the thermal boundary layer grow to the thickness defined by the chemical boundary layer. Because thermal relaxation ultimately stops at a maximum thickness defined by the chemical boundary layer, continents eventually come to reside at a terminal resting elevation for a given ambient mantle temperature.

Secular cooling of the earth’s mantle requires emergence of continents

Equation (2) shows that the terminal resting elevation of a stable continent is not only controlled by thermal boundary layer thickness ($h_{cc} + h_{cr}$) but also by mantle potential temperature T_m (Figure 2(b)). For continental thermal boundary layers that have relaxed to their maximum thicknesses, the total thermal buoyancy associated with the mantle root will vary as the temperature of the convecting mantle varies (Equations (1) and (2)), assuming that the temperature at the base of the continental thermal boundary layer is equivalent to the temperature of the Earth’s convecting mantle and that the continental thermal boundary layer itself is fixed by the thickness of the chemical boundary layer. For a fixed thickness chemical boundary layer, the relative effect of thermal contraction is higher when the Earth is hot, so stable continents ride low when the Earth is hot (Figure 4(a)). In a colder mantle, when the relative effect of thermal contraction decreases and the negative buoyancy of the mantle root is smaller, stable continents ride higher (Figure 4(a)). This concept is laid out in Equation (2) and illustrated graphically in Figure 4(a), where it can be seen that the integrated negative thermal buoyancy represents the triangular area between the geotherm and the mantle adiabat. If

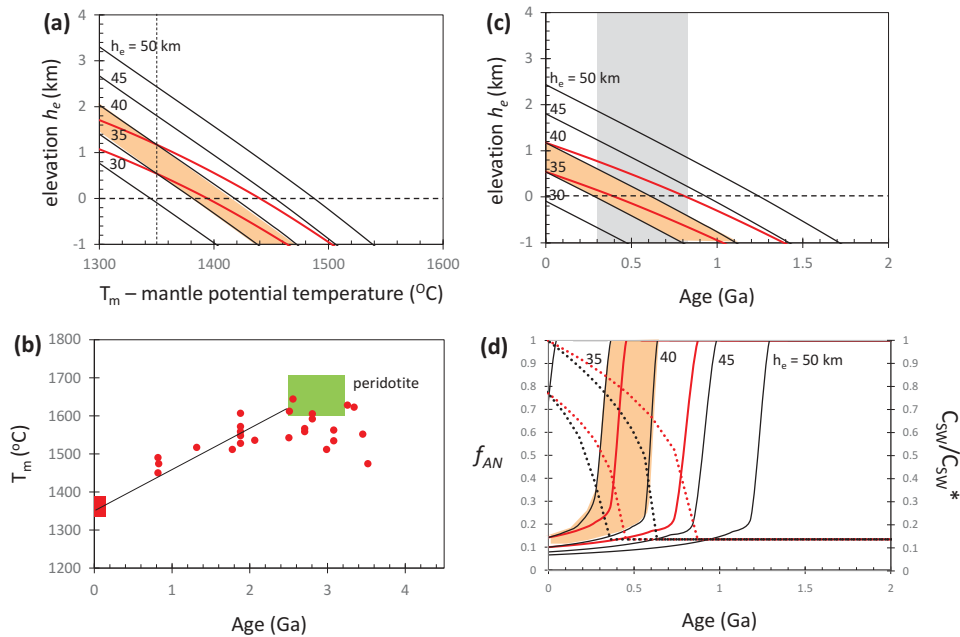


Figure 4. (a) Continental elevation h_e versus mantle potential temperature T_m contoured against continental crust thickness h_{cc} . Present day mantle potential temperature shown by vertical dashed line. Solid black lines correspond to mobile plate convective regime ($n = 0.6$) for h_e at 5 km intervals (orange shaded area for 35–40 km). Solid red line for strong plate regime ($n = 0.2$) for 35 and 40 km only. (b) Mantle potential temperature (T_m) versus time. Red symbols correspond to mantle temperature constraints based on basalt thermometry (Putirka 2005; Herzberg *et al.* 2007; Lee *et al.* 2009; Lee and Chin 2014). Green box represents temperatures estimated from residual cratonic peridotites (Herzberg and Rudnick 2012; Lee and Chin 2014). Solid black line represents assumed thermal evolution since 2.5 Ga (c). Terminal resting elevations of stable continents as a function of time (Ga), using the observed secular variation in mantle temperature (b) as a constraint. Solid black lines are calculated for a mobile plate regime for different crustal thicknesses at 5 km intervals (orange shaded region corresponds to 35–40 km). Solid red line corresponds to a strong plate regime for crustal thickness of only 35 and 40 km. Typical crustal thickness of stabilized continental interiors is ~35–40 km, which corresponds to a global emergence of continents between 0.4 and 1.1 Ga (billion years ago). (d) Solid black lines (mobile lid regime) and left-hand axis refer to fraction of continental seas relative to total continental area, which we use as a proxy for fractional area of anoxic sedimentation f_{AN} (models are the same as in (a)–(c)). Red solid lines are for rigid plate regime for 30 and 40 km thick crust only. Dashed lines and right-hand axis correspond to increase in seawater concentration of phosphorous (P) relative to present day due to a decrease in f_{AN} . Cases for 35 and 40 km only are shown (black is for mobile plate and red is for strong plate). It is assumed that 70% of P is sequestered today in anoxic margins, which are assumed to make up 10% of the present continental area. Mantle root thickness is assumed to 175 km in all above models.

the mantle is hotter, than the total negative thermal buoyancy is larger than in a cold mantle, and thus, continents of fixed thermal boundary layer thickness ride lower in hot mantle and high in a cold mantle. This sensitivity to mantle potential temperature is consistent with the results of other studies (Galer 1991; Vlaar 2000; Flament *et al.* 2008).

The Earth's convecting mantle appears to have cooled. Thermobarometric constraints on basalt and cratonic peridotite melting temperatures suggest potential temperatures of 1500–1700°C in the late Archaean (Figure 4(b)) (Herzberg *et al.* 2010; Herzberg and Rudnick 2012; Lee and Chin 2014). Present day mantle potential temperatures, based on thermometry of mid-ocean ridge basalts and abyssal peridotites, are suggested to be 1350–1400°C (Putirka 2005; Herzberg *et al.* 2007; Lee *et al.* 2009; Lee and Chin 2014). Thus, since 2.5 Ga, the convecting mantle may have cooled

by 200°C. We adopt a linear fit for cooling since 2.5 Ga of $T = 1350 + 110t$, where T is in Celsius and t is in Ga.

Taking these constraints on how T_m has changed since 2.7 Ga, the terminal resting elevation of continents with time can be evaluated. We modified the above equations to include the effects of the ocean as well as the effects of mantle temperature on oceanic crust thickness and oceanic thermal boundary layer thickness; the latter is controlled by average oceanic plate velocity and age, which depends on the nature of convection (see Appendix). We have assumed that ocean mass and continental area have not changed significantly since 2.7 Ga (see Appendix). The first assumption is likely reasonable given that there are inherent negative feedbacks in the whole-Earth water cycle that drive the oceans to steady state within a few hundred million years (McGovern and Schubert 1989; Sandu *et al.* 2011). At least 50% of the present mass of

continents may have already formed by late Archaean times and >80% by the end of the Proterozoic based on Nd and Sr isotopes (Jacobsen 1988; Dhuime *et al.* 2012); within this range, our model calculations are not so sensitive to continental area.

Our models predict that continents emerge as the Earth cools. This trend agrees with previous work (Galer 1991; Vlaar 2000; Flament *et al.* 2008), but differs in that those studies predicted emergence in the late Archaean or early Proterozoic. For continents having crustal thicknesses between 35–40 km and chemical boundary layer thicknesses of ~150 km, our model predicts emergence to occur much later, anywhere between 800–300 Ma (Figure 4(c)). We cannot be more precise in our predictions because the timing depends on assumed compositional density structure and convection parameters, the latter which dictate the average age of oceanic plates (Figure 4(c)). Further, it is likely that the major cratons emerged diachronously during this period, given different formation times and structures. What is different in our model is that we have accounted for the presence of a continental thermal boundary layer whose thickness is defined by the presence of a permanent chemical boundary layer, which is not isopycnic but instead exhibits a net negative thermal buoyancy.

Late emergence may seem at odds with evidence for siliclastic sediments in the Archaean and Proterozoic, which would seem to require areas of emergent crust. For most of Earth's history, we envision a water world characterized by oceanic and continental seas. Regions of land would still exist, but they would be represented by narrow, high-standing belts of active volcanic arcs and continental collisions. These 'islands' would serve as the source of siliclastic sediments, but the remaining parts of the continents – the stable portions – would have been below sea level. As mantle temperature decreased with time, continental buoyancy increased, causing stable continents to gradually rise. Our calculations predict widespread emergence sometime in the Late Proterozoic (Figure 4(a)).

Unstable climate during emergence

Continent elevation could have an indirect effect on Earth's climate through effects on the generation of ice sheets and the ice-albedo feedback. In a water world, large, permanent ice sheets are difficult to form (Pierrehumbert 2010) as large ice sheets more readily form on continents. Could the transition from a water world to a terrestrial world have marked the transition from a relatively ice-free to ice-prone world, with implications for Earth's climatic evolution? It is widely accepted that very high levels of greenhouse gases

(e.g. CO₂) are required to maintain liquid water on the Earth's surface in light of the sun's 30% lower luminosity in the Archaean and Proterozoic (Sagan and Mullen 1972; Feulner 2012). However, the inability to form permanent ice sheets in a water world would help to maintain a lower albedo, relaxing the requirement for exceptionally high atmospheric CO₂ concentrations in the Archaean (Feulner 2012). Importantly, the strength of an ice-albedo feedback in the Archaean and early Proterozoic would be substantially diminished because permanent ice would largely only form on the thin strips of subaerial mountains. Indeed, the evidence for Archaean and Palaeoproterozoic glaciations (Evans *et al.* 1997; Young *et al.* 1998) may reflect these mountain glaciers rather than extensive, global ice sheets.

Because continents are mostly flat, continental land surface area can grow rapidly during emergence, perhaps within a time interval of less than 200 million years (Figure 4(d)). Prior to emergence, ~30% of Earth's surface would be characterized by shallow seas, but immediately after emergence, shallow continental seas would shrink rapidly to a narrow ribbon of continental shelves on the margins of emerged continents. Near the threshold between water-world and terrestrial world, total continental area would be sensitive to regional tectonics and higher frequency glacio-eustatic effects, causing the planet to switch back and forth between a water world and terrestrial world. We would expect climatic conditions on Earth during the transition to be highly unstable, perhaps flipping back and forth between ice-free and ice-house conditions due to the differences in ice-albedo feedbacks between land and water. The occurrence of several long-lived Snowball events in the Neoproterozoic could be a manifestation of this predicted climate instability (Hoffman and Schrag 2002).

Change in the nature of continental weathering

Emergence would have also altered the nature of continental weathering. In a water-world, continental weathering would have been confined primarily to regions undergoing active orogenesis, thereby involving more geochemically juvenile crust. Though the high relief and reactivity of these rocks would promote efficient weathering (Maher and Chamberlain 2014), these subaerial regions would occupy only a fraction of the Earth's surface, suggesting that quantitatively, these regions may not have contributed significantly to weathering on a global scale. Further, these regions may have efficiently exported sediment to the submerged, continental basins, in which weathering is thought to be suppressed. Instead, in a water world, chemical weathering would have occurred primarily at

mid-ocean ridges and in oceanic crust (Coogan and Gillis 2013; Mills *et al.* 2014; Coogan and Dosso 2015).

After emergence, weathering would commence across the broad low relief surfaces of the continents, which had previously served as depocentres for ancient sediments during water world times. Emergence would usher the Earth into a new regime in which re-weathering or re-working of ancient sediments becomes important. The fact that the largest rise in the seawater record of radiogenic strontium isotopes ($^{87}\text{Sr}/^{86}\text{Sr}$) occurred around 700 Ma and remained relatively high to the present day (Prokoph *et al.* 2008) (Figure 5(a)), has always been perplexing, but is consistent with a rapid and irreversible transition to weathering of older sediments on the continents as a consequence of late emergence.

The consequences of a shift from primarily oceanic/ seafloor basalt weathering to primarily terrestrial weathering would be dramatic (Mills *et al.* 2014).

Seafloor basalt weathering (F_{sbw}) is typically modelled as a n -th-order reaction, with an exponent of 0.2–0.25 (Godderis and Francois 1995; Brady and Gislason, 1997; Mills *et al.* 2014) such that:

$$F_{sbw} = k[R_{\text{CO}_2}]^n \quad (4)$$

where k is a proportionality constant, R_{CO_2} is the ratio of $p\text{CO}_2$ at time t relative to modern pre-industrial, and n accounts for a non-linear response between climate and F_{sbw} . In contrast, terrestrial chemical weathering is thought to be characterized by an n of 0.6 or greater (Volk 1989; Berner 2004) (see also discussion in Caves *et al.* (2016)). At constant inputs of CO_2 , an Earth system characterized by $n = 0.2$ permits higher atmospheric CO_2 than one characterized by $n = 0.6$. Thus, as continents emerged, weathering would briefly increase above the input level of CO_2 , dramatically reducing

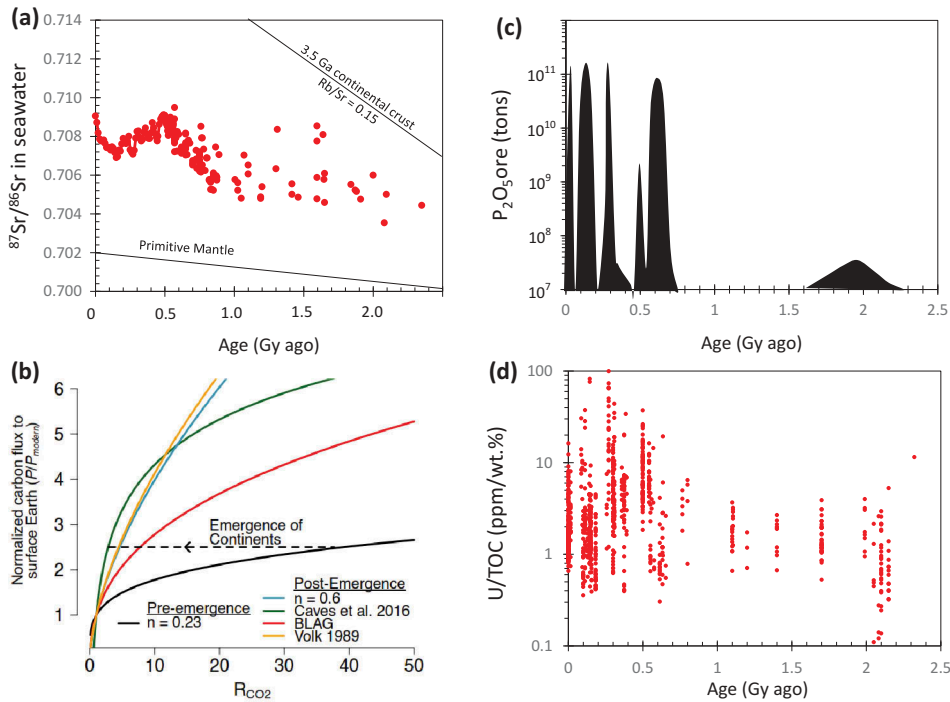


Figure 5. (a) Carbonate $^{87}\text{Sr}/^{86}\text{Sr}$, a proxy for seawater strontium isotopes, plotted versus time. Lower diagonal line represents the time-integrated ingrowth of ^{87}Sr for the primitive mantle (Prokoph *et al.* 2008). Upper diagonal line represents the closed system ingrowth for that of typical continental crust with elemental Rb/Sr ratio of 0.15, formed 3 Ga. Marked transition in Neoproterozoic times from unradiogenic to radiogenic states indicates a fundamental change in weathering regime, which we attribute to emergence of continents and re-weathering of ancient sediments. (b) Comparison of hypothesized weathering feedbacks pre- and post-emergence. Pre-continental emergence Earth would be characterized by dominantly seafloor basalt weathering, which has a feedback strength with $n = 0.23$ (see Equation (4)). Post-continental emergence Earth is characterized by a stronger feedback. Shown are estimates for the strength of the weathering feedback during the Phanerozoic. Though there is disagreement regarding the precise functional form of the Phanerozoic weathering feedbacks, all of the Phanerozoic weathering feedbacks permit lower CO_2 at a given input flux of carbon than does the pre-emergence feedback. Thus, continental emergence would shift the atmosphere toward lower $p\text{CO}_2$, even at the same input flux of carbon. Note that these equations assume steady state in the surface Earth carbon cycle (i.e. inputs from volcanism and organic C oxidation equal outputs from silicate weathering and organic C burial) (Berner and Caldeira 1997; Caves *et al.* 2016). R_{CO_2} is the ratio of $p\text{CO}_2$ to modern pre-industrial $p\text{CO}_2$. P is the flux of C from the solid Earth to the surface Earth. (c) Tonnage of phosphorous ore deposits (P_2O_5) versus time (Pufahl and Hiatt 2012). (d) Uranium concentrations (ppm) of shales as a function of time, normalized to total organic carbon content (wt. %) (Lyons *et al.* 2014).

the level of atmospheric CO₂, until a new steady-state is achieved (Figure 5(b)).

This effect would act as a positive feedback that would amplify the land-ice albedo feedback already discussed above, further accentuating climate instability during the period in which continents were intermittently submerged and exposed. For example, as small amounts of ice formed – reducing sea-level and exposing a greater area of the continents – weathering would transition from the relatively inefficient weathering of seafloor basalts to increasingly continental weathering (Figure 5(b)). This would reduce CO₂ further, leading to greater continental ice and further lowering of sea-level.

Accompanying this change in weathering would be a change in the hydrologic cycle. The generation of large regions of land would initiate a strong freshwater hydrologic cycle in the form of continental ice sheets and groundwater. It is well known that the oxygen isotopic composition of fresh water becomes lighter with increasing continentality (Rozanski *et al.* 1993; Winnick *et al.* 2014), so a pronounced freshwater hydrologic cycle might be manifested in terms of lighter oxygen isotopic compositions of continental weathering products, such as clays in shales. Compilations of the oxygen isotopic compositions of shales show a gradual secular increase since the Archaean, presumably due to the accumulating effects of weathering and sedimentation on the continents (Bindeman *et al.* 2016). This increase matches the increase in δ¹⁸O in marine cherts and carbonates (Prokoph *et al.* 2008). However, after ~1 Ga, the rise in shale δ¹⁸O slows relative to the continued and accelerated increase in cherts and carbonates (Bindeman *et al.* 2016). While other effects may also explain the increasing divergence between terrestrially-derived shales and marine cherts and carbonates, such a change would be expected by an increase in subaerial continental weathering.

Biogeochemical cycling, oxygenation, and the Cambrian explosion

Carbonates and organic carbon are preferentially deposited in shallow seas, the former because calcium carbonate dissolves in deep waters due to the cold temperatures at depth that increase calcite solubility, and the latter because shallow waters provide less time for sinking organic material to oxidize (Ridgwell and Zeebe 2005). Prior to emergence, most of the carbon released from the Earth's interior by volcanism, would be stored on continents, leaving only a small fraction exported to the deep ocean. Carbon would have

accumulated on the continents over time, with only small amounts of carbon being subducted (Lee *et al.* 2013). After emergence, when the area of shallow seas diminishes, a larger fraction of the global carbon output from the ocean/atmosphere system would have migrated to the deep oceans. However, it is not until the Mesozoic – at least 250 million year following the predicted large-scale emergence of the continents – that pelagic calcifiers evolve and provide an efficient method of exporting carbon to the deep-ocean (Ridgwell 2005). Thus, the period between widespread continental submergence and evolution of pelagic calcifiers would have been a curious period in Earth history, with limited extents of shallow seas, but with export of carbonate to the deep-ocean primarily occurring as mass-wasting off of carbonate shelves (Milliman and Droxler 1996). The enforced limitation of carbonate burial to areally-limited shelves may explain the widespread and thick shallow-ocean carbonate accumulations characteristic of the Palaeozoic (Walker *et al.* 2002). The eventual increase in deep-ocean carbonate burial would have possibly initiated, for the first time in Earth's history, significant recycling of carbon into the mantle through subduction zones.

Similar implications follow for the cycling of nutrients like P, as well as redox-sensitive elements, such as Mo and U (Figure 5(c,d)). These elements are scavenged or preserved where organic carbon is preserved and buried (Lyons *et al.* 2009) (Figure 6(a,c)). Organic C is preferentially buried in shallow seas where the oxygen minimum zone intersects the sediment-water interface (Figure 6). Thus, contraction of shallow seas from the continental scale to the narrow shelves of the modern world, would cause an increase in seawater P concentration (C_{sw}) (Ozaki and Tajika 2013) (Figure 6). Assuming steady state, where input of P (mainly riverine) is balanced by burial outputs, this mass balance is given by:

$$\frac{C_{sw}}{C_{sw}^*} = \frac{J_{in} D_{an} f_{an}^* X_{cc}^* + D_{ox}(1 - X_{cc}^*)}{J_{in}^* D_{an} f_{an} X_{cc} + D_{ox}(1 - X_{cc})}, \quad (5)$$

where J_{in} is the riverine input (moles/year) of dissolved P, X_{cc} is the surface area fraction of continents on Earth (0.3), $1 - X_{cc}$ is the surface area fraction of deep ocean basins (0.7), f_{an} is the fraction of continental surface area that is submerged, D_{an} and D_{ox} are effective rate constants for P burial flux in anoxic and oxic environments, and asterisks '*' reflects present day conditions. In the above, we define continents as anything that lies above the deep ocean basin, with total submergence of continents corresponding to $f_{an} = 1$. Today, only a small fraction f_{an}^* of the continental shelves is submerged. We assume that continental seas are shallow and represented by anoxic or suboxic conditions while

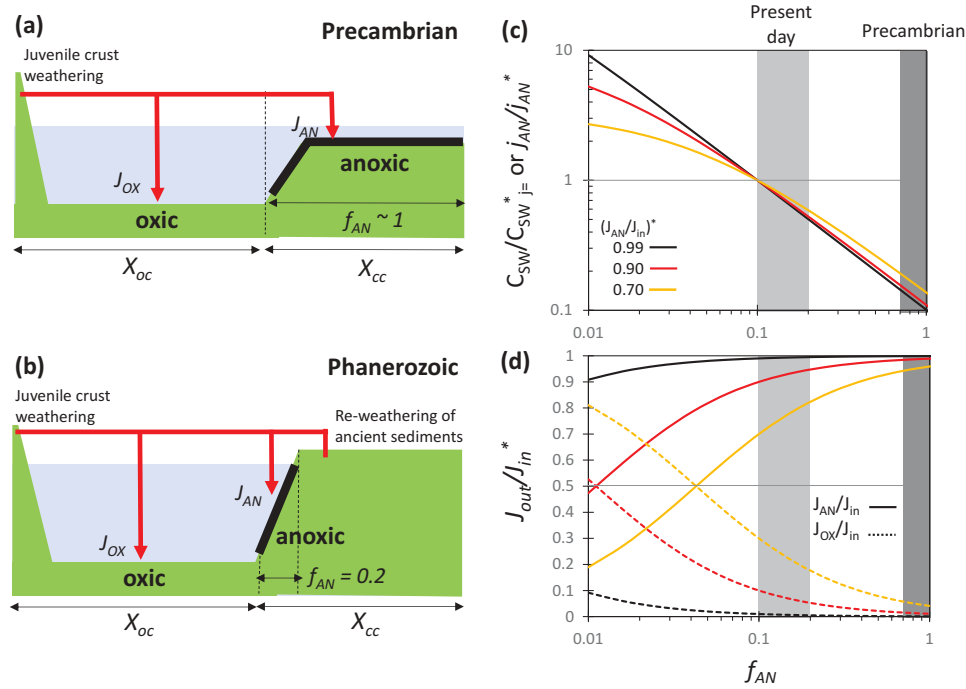


Figure 6. (a) and (b) Cartoons of inputs and outputs of an element that partitions differently between anoxic (shallow continental seas) and oxic (deep ocean) settings, such as phosphorous (P). Horizontal red line represents weathering input of P. Vertical arrows represent *total* P outputs (moles/year) into oxic J_{OX} and anoxic sediments J_{AN} . In Precambrian setting A, stable continents are below sea level, but in Phanerozoic, continents are mostly above sea level. In all cases, regions of active crust formation, are assumed to be above sea-level. In Precambrian times, weathering of juvenile crust is dominant source of P input to ocean, but in the Phanerozoic, re-weathering of ancient sediments stored on the continents amplifies total inputs of P. Emergence of continents results in a substantial decrease in area of shallow seas (f_{AN} decreases). (c) Vertical axis represents seawater concentration of an element relative to modern day (*), or equivalently, the output flux j (moles/cm²/year) in anoxic (j_{AN}) or oxic sediments (j_{OX}) relative to present day. Horizontal axis represents fraction of continents submerged, assumed to be anoxic f_{AN} . Model curves correspond to different assumed proportions of P buried in anoxic sediments today J_{AN}/J_{in}^* with a value of 50–80% corresponding to P today. Values of 99%, 90%, and 70% are shown for comparison. Continental area is assumed to be 30% of the surface of the Earth and the modern area of anoxic sedimentation (relative to continental area) is assumed to be 10%. (d) Same model outputs as in C, but proportion of total output into anoxic J_{AN}/J_{in} and oxic J_{OX}/J_{in} are shown with solid and dashed lines, respectively, as a function of anoxic sedimentation areal fraction f_{AN} (relative to continental area). As f_{AN} decreases, total output of P into anoxic sediments decreases while output into oxic sediments increases. However, the flux of P into anoxic sediments and the concentration of seawater P both increase as f_{AN} decreases, as shown in (c).

the deep ocean is reflected by oxic conditions. The rate constants are calibrated using the present day burial efficiency of P in anoxic and oxic basins (at least 50–80% of P is buried on continental shelves today (Filippelli 2002; Rutenberg 2003)), that is, $D_{an} = j_{an}^*/M_{sw}^*$ and $D_{ox} = j_{ox}^*/M_{sw}^*$, where j_i represents burial flux (moles/cm²/year) and M represents the mass of P in the oceans, such that the rate constants have units of cm⁻²year⁻¹. Assuming that the rate constants and area of continents have not changed significantly in time, it can be seen from Equation (5) that decreasing f_{an} leads to an increase in P concentration in seawater (Figures 4 (d) and 6(c)). This increases the area-integrated output (moles/year) of P into the oxic deep oceans and decreases the outputs in anoxic shallow seas, but increases the actual flux (P burial rate *per unit area*) in the anoxic shallow seas (Figure 6(c,d)). By contrast,

increasing the area of shallow seas, reduces the amount of P in seawater, increases the *total* output of P from shallow seas, but decreases the burial flux of P in shallow seas, owing to dilution (Figure 6(c,d)). The emergence of continents should have led to an increase in seawater P and in the concentration of P in anoxic sediments by simply changing the efficiency by which P is buried in marine environments (Figures 4(d) and 6(c)). Post-emergence P availability would have been further enhanced by the onset of continental weathering (e.g. increasing J_{in} in Equation (5)) due to the added contribution from re-working of ancient sediments, themselves enriched in P relative to juvenile igneous rocks. Our predictions are consistent with the observation that the frequency of phosphorite deposits increased markedly after 700 Ma (Pufahl and Hiatt 2012) (Figure 5(c)). The rise in U concentrations of black shales after 700 Ma (Figure 5(d)) can

Table 1. Definitions of symbols and variables.

ρ_w	Density of seawater (kg/m ³)
ρ_{cc}	Density of continental crust (kg/m ³)
ρ_{cr}	Density of continental lithospheric mantle (kg/m ³)
ρ_{oc}	Density of oceanic crust (kg/m ³)
ρ_{or}	Density of oceanic lithospheric mantle (kg/m ³)
ρ_a	Density of asthenospheric mantle (kg/m ³)
ρ_w^0	STP density of seawater (1030 kg/m ³)
ρ_{cc}^0	STP density of continental crust (2900 kg/m ³)
ρ_{cr}^0	STP density of continental lithospheric mantle (3350 kg/m ³)
ρ_{oc}^0	STP density of oceanic crust (2900 kg/m ³)
ρ_{or}^0	STP density of oceanic lithospheric mantle (3370 kg/m ³)
ρ_a	STP density of asthenospheric mantle (3380 kg/m ³)
h_e	Elevation above sea level (m)
h_{ow}	Depth of ocean basin (m)
h_{cc}	Thickness of continental crust (m)
h_{cr}	Thickness of continental lithospheric mantle root (m)
h_{oc}	Thickness of oceanic crust (m)
h_{or}	Thickness of oceanic lithospheric mantle root (m)
h_e	Elevation of continental crust above sea level (m)
h_{cw}	Depth of continents below sea level if continents are completely submerged (m)
V_w	Global volume of ocean water (m ³)
h_{ow}^*	Present day average depth of oceans (4.3 km)
A_{oc}^*	Present day area of ocean crust (km ²)
A_{cc}	Area of continental crust (km ²)
A_{oc}	Area of oceanic crust (km ²)
T_i	Temperature of a given layer (°C)
ρ_i^0	Density of a given layer at standard state and pressure (kg/m ³)
α	Thermal expansivity ($3 \times 10^{-5}/^\circ\text{C}$)
T_m	Mantle potential temperature (°C)
K	Thermal diffusivity (10^{-6} m ² /s)
τ_{oc}	Average residence time of oceanic crust at surface of the Earth (million years)
τ^*	average modern residence time of oceanic crust at surface of the Earth (80 million years)
u^*	Average modern oceanic plate velocity (m/y)
u	Average oceanic plate velocity (m/y)
T_m^*	Modern mantle potential temperature (°C)
η^*	Average viscosity of the modern mantle (Pa s)
η	Average viscosity of the mantle
n	Exponent in Eq. A9 (0.2–0.66)
E	Activation energy (350 kJ/mol)
R	Gas constant
$\frac{dh_{cc}}{dt}$	Rate of change in crustal thickness (m/y)
M	Crustal thickening rate (m/y)
E	erosion rate (m/y)
k_e	Erosion rate constant or efficiency of erosion (1/y)
t	time (y)
J_{in}	Global elemental input rate into oceans (moles/year)
J_{ox}	Global elemental output rate from oceans in oxic sediments (moles/year)
J_{an}	Global elemental output rate from oceans in anoxic/suboxic sediments (moles/year)
j_{ox}	Flux of elemental output in oxic sediments (moles/m ² /year)
j_{an}	Flux of elemental output in anoxic/suboxic sediments (moles/m ² /year)
f_{an}	Fraction of continental area that is submerged
D_{an}	Partition coefficient for burial of element in anoxic/suboxic sediments (cm ⁻² year ⁻¹)
D_{ox}	Partition coefficient for burial of element in oxic sediments (cm ⁻² year ⁻¹)
C_{ow}	Total mass of element in the oceans
J_{an}^*/J_{in}^*	Fraction of element buried in anoxic/suboxic sediments today
J_{ox}^*/J_{in}^*	Fraction of element buried in anoxic/suboxic sediments today
X_{cc}	Fraction of continental crust area relative to surface area of Earth
$(1-X_{cc})$	Fraction of oceanic crust area relative to surface area of Earth
y	Elevation of continental crust <i>relative</i> to the bottom of the ocean
f	Fractional area relative to the continental crust ($0 < f < 1$)
b	Approximate width of continental margin (m)

be explained similarly (Lyons *et al.* 2014). Our conclusions are consistent with recent suggestion that Archaean and Proterozoic oceans were P-limited and only became more replete after the Neoproterozoic (Reinhard *et al.* 2017). Greater availability of P after Neoproterozoic emergence may have enhanced biological productivity.

Finally, the emergence of continents may have also played a role in the evolution of atmospheric oxygen. Higher biological productivity may have resulted in more efficient burial of organic carbon, which would have increased oxygen production, possibly allowing atmospheric oxygen to rise irreversibly in Neoproterozoic times (not to be confused with the

Palaeoproterozoic rise in oxygen around 2.3 Ga). Recently, Lee et al. showed that the steady build-up of carbonates on continental margins through time would have indirectly amplified volcanic degassing of carbon dioxide through metamorphic and magmatically induced decarbonation of the ever-growing reservoir of continental carbonates, in turn enhancing photosynthetic oxygen production (Lee et al. 2013, 2016). In both scenarios, the effect of continents in modifying carbon storage and nutrient availability predict late atmospheric oxygenation. Because oxygen availability removes limits in animal body size and enhances trophic complexity in carnivorous organisms (Knoll and Carroll 1999; Schiffbauer et al. 2016), it is tempting to speculate that the Cambrian explosion of animal diversity was driven by deep Earth processes, manifested through the changing expression of continents through time. Recent studies have shown that the Cambrian diversification did not occur as an abrupt 'explosion' but rather occurred over an extended interval of time (Schiffbauer et al. 2016), consistent with a deep Earth driver.

Caveats

We recognize that our entire analysis is clearly speculative and highly model-dependent, but we present it as a possible scenario for Earth's evolution. We note that even though our predictions of Neoproterozoic emergence can explain many of unusual geologic phenomena during that time, our conclusions seem to contradict some studies. For example, Peters and Gaines (2012) interpreted the rise in $^{87}\text{Sr}/^{86}\text{Sr}$ in the Neoproterozoic to represent large-scale inundation or submergence of continents, wherein waves erode the veneer of sediments on continents as subsidence occurs. However, wave-based erosion would generate the same effect during emergence. We note that the inundated continental margins in the Palaeozoic could reflect part of a protracted transition towards emergence or they could represent the effects of dynamic topography, which would be superimposed on the secular change associated with cooling of the Earth argued here.

The most serious uncertainty is whether ocean volume has changed significantly with time. Korenaga et al. (2016) performed a more sophisticated analysis than ours by designating ocean volume and continental area as variables while assuming constant continental freeboard through time. In our model, we have assumed ocean volume to be constant and continental area since the end of the Archaean to be constant. They concluded that continents emerged in the late

Archaean, much earlier than predicted by our study, and that continents might even have re-submerged in the Phanerozoic. Their model also predicts a rise in seawater $^{87}\text{Sr}/^{86}\text{Sr}$ due to continental emergence, but no significant increase occurs in the late Archaean or Palaeoproterozoic. The authors noted, however, that their models are consistent with changes in the abundance of terrestrial and marine formations, with preserved marine formations being more prevalent in the Phanerozoic. Whether the sedimentary record is truly representative of the past given preservation bias remains to be seen. In summary, both the Korenaga et al. and our analyses are fundamentally based on models, so it is also possible that both of us are wrong. More important is that these models provide some sense of how the Earth system should evolve. If ocean volume and continental area have not changed significantly, our model predicts that stabilized continents should emerge as the Earth cools, but exactly when is dependent on a number of assumptions.

Conclusions

The history of a continent begins with orogeny, followed by a long period of maturation, subsidence and eventual submergence. Initially, the Earth must have been a water world, with deep ocean basins and shallow continental seas. Regions of land were confined to narrow belts defined by active orogenic belts. The submerged stable parts of continents served as efficient repositories of sediments as well as for key redox-sensitive elements and nutrients. As the Earth's interior cooled, continents gradually rose, culminating in rapid emergence, through fits and starts and possible instabilities in climate during the Late Proterozoic. Emergence led to irreversible changes in marine biogeochemical cycling, continental weathering and the global hydrologic cycle, which collectively served as a backdrop for the Cambrian explosion of animals. Although the exact timing of emergence in our models is unclear, what is clear is that the irreversible cooling of the Earth leads inevitably to continental emergence, permanently changing how the Earth's surface operates.

Acknowledgements

The topic of unconformities was inspired by discussions with Albert W. Bally, John Anderson's sedimentology course, papers by Dan McKenzie and Peter Sadler, and early geology outings with Tien Lee, Zora Lee and Douglas Morton. Interest in anoxic sediments and phosphorous came from Gerald Wasserburg. Discussions with Sally Thurner, Eugene

Humphreys, Dave Snyder, Shijie Zhong, Gary Gray, Lexi Malouta, Elli Ronay, C. Page Chamberlain, Kevin Boyce, and members of Rice Loony NoonZ helped crystallize our thoughts. This paper is dedicated to Richard J. O'Connell and Gerald Wasserburg for their ability to de-complicate nature. This work was supported by the NSF Frontiers of Earth System Dynamics (OCE-1338842) and represents a contribution from the Continental-Island Arc (CIA) working group.

Disclosure statement

No potential conflict of interest was reported by the authors.

Funding

This work was supported by the National Science Foundation [OCE-1338842].

References

- Artemieva, I.M., and Mooney, W.D., 2001, Thermal thickness and evolution of Precambrian lithosphere: A global study: *Journal of Geophysical Research: Solid Earth*, v. 106, p. 16387–16414. doi:10.1029/2000JB900439
- Berner, R.A., 2004, *The Phanerozoic carbon cycle: CO₂ and O₂*: Oxford, Oxford University Press.
- Berner, R.A., and Caldeira, K., 1997, The need for mass balance and feedback in the geochemical carbon cycle: *Geology*, v. 25, p. 955–956. doi:10.1130/0091-7613(1997)025<0955:TNFMBA>2.3.CO;2
- Bindeman, I.N., Bekker, A., and Zakharov, D.O., 2016, Oxygen isotope perspective on crustal evolution on early Earth: A record of Precambrian shales with emphasis on Paleoproterozoic glaciations and Great Oxygenation event: *Earth and Planetary Science Letters*, v. 437, p. 101–113. doi:10.1016/j.epsl.2015.12.029
- Brady, P.V., and Gislason, S.R., 1997, Seafloor weathering controls on atmospheric CO₂ and global climate: *Geochimica et Cosmochimica Acta*, v. 61, p. 965–973. doi:10.1016/S0016-7037(96)00385-7
- Brocher, T.M., 2005, Empirical relations between elastic wave-speeds and density in the Earth's crust: *Bulletin of the Seismological Society of America*, v. 95, p. 2081–2092. doi:10.1785/0120050077
- Caves, J.K., Jost, A.B., Lau, K.V., and Maher, K., 2016, Cenozoic carbon cycle imbalances and a variable weathering feedback: *Earth and Planetary Science Letters*, v. 450, p. 152–163. doi:10.1016/j.epsl.2016.06.035
- Coogan, L.A., and Dosso, S.E., 2015, Alteration of ocean crust provides a strong temperature dependent feedback on the geological carbon cycle and is a primary driver of the Sr-isotopic composition of seawater: *Earth and Planetary Science Letters*, v. 415, p. 38–46. doi:10.1016/j.epsl.2015.01.027
- Coogan, L.A., and Gillis, K.M., 2013, Evidence that low-temperature oceanic hydrothermal systems play an important role in the silicate-carbonate weathering cycle and long-term climate regulation: *Geochemistry, Geophysics, Geosystems*, v. 14, p. 1771–1786. doi:10.1002/ggge.v14.6
- Cooper, C.M., Lenardic, A., Levander, A., and Moresi, L., 2006, Creation and preservation of cratonic lithosphere: Seismic constraints and geodynamic models: *AGU Monograph*, v. 164, p. 75–88.
- Cooper, C.M., Lenardic, A., and Moresi, L., 2004, The thermal structure of stable continental lithosphere within a dynamic mantle: *Earth and Planetary Science Letters*, v. 222, p. 807–817. doi:10.1016/j.epsl.2004.04.008
- Dhuime, B., Hawkesworth, C.J., Cawood, P.A., and Storey, C.D., 2012, A change in the geodynamics of continental growth 3 billion years ago: *Science*, v. 335, p. 1334–1336. doi:10.1126/science.1216066
- Eriksson, P.G., Mazumder, R., Catuneanu, O., Bumby, A.J., and Ilondo, B.O., 2006, Precambrian continental freeboard and geological evolution: A time perspective: *Earth-Science Reviews*, v. 79, p. 165–204. doi:10.1016/j.earscirev.2006.07.001
- Evans, D.A., Beukes, N.J., and Kirschvink, J.L., 1997, Low-latitude glaciation in the Palaeoproterozoic era: *Nature*, v. 386, p. 262–266. doi:10.1038/386262a0
- Ewing, M., and Press, F., 1955, Geophysical contrasts between continents and ocean basins: *Geological Society of America Special Papers*, v. 62, p. 1–6.
- Feulner, G., 2012, The faint young sun problem: *Reviews of Geophysics*, v. 50, p. RG2006. doi:10.1029/2011RG000375
- Filippelli, G.M., 2002, The global phosphorous cycle: *Reviews of Mineralogy and Geochemistry*, v. 48, p. 391–425.
- Fischer, K.M., 2002, Waning buoyancy in the crustal roots of old mountains: *Nature*, v. 417, p. 933–936. doi:10.1038/nature00855
- Flament, N., Coltice, N., and Rey, P.F., 2008, A case for late-Archaean continental emergence from thermal evolution models and hypsometry: *Earth and Planetary Science Letters*, v. 275, p. 326–336. doi:10.1016/j.epsl.2008.08.029
- Fliedner, M.M., and Klempner, S.L., 2000, Crustal structure transition from oceanic arc to continental arc, eastern Aleutian Islands and Alaska Peninsula: *Earth and Planetary Science Letters*, v. 179, p. 567–579. doi:10.1016/S0012-821X(00)00142-4
- Flowers, R.M., Bowring, S.A., and Reiners, P.W., 2006, Low long-term erosion rates and extreme continental stability documented by ancient (U-Th)/He dates: *Geology*, v. 34, p. 925–928. doi:10.1130/G22670A.1
- Galer, S.J.G., and Mezger, K., 1998, Metamorphism, Denudation And Sea Level In The Archean And Cooling Of The Earth: *Precambrian Research*, v. 92, p. 389–412. doi:10.1016/S0301-9268(98)00083-7
- Galer, S.J.G., 1991, Interrelationships between continental freeboard, tectonics and mantle temperature: *Earth and Planetary Science Letters*, v. 105, p. 214–228. doi:10.1016/0012-821X(91)90132-2
- Godderis, Y., and Francois, L.M., 1995, The Cenozoic evolution of the strontium and carbon cycles: Relative importance of continental erosion and mantle exchanges: *Chemical Geology*, v. 126, p. 169–190. doi:10.1016/0009-2541(95)00117-3
- Gung, Y., Panning, M., and Romanowicz, B., 2003, Global anisotropy and the thickness of continents: *Nature*, v. 422, p. 707–711. doi:10.1038/nature01559
- Hasterock, D., and Chapman, D.S., 2007, Continental thermal isostasy: 1. Methods and sensitivity: *Journal of Geophysical Research*, v. 112. doi:10.1029/2006JB004663
- Herzberg, C., Asimow, P.D., Arndt, N.T., Niu, Y., Leshner, C.M., Fitton, J.G., Cheadle, M.J., and Saunders, A.D., 2007,

- Temperatures in ambient mantle and plumes: Constraints from basalts, picrites and komatiites: *Geochemistry, Geophysics, Geosystems*, v. 8. doi:10.1029/2006GC001390
- Herzberg, C., Condie, K.C., and Korenaga, J., 2010, Thermal history of the Earth and its petrological expression: *Earth and Planetary Science Letters*, v. 292, p. 79–88. doi:10.1016/j.epsl.2010.01.022
- Herzberg, C., and Rudnick, R.L., 2012, Formation of cratonic lithosphere: An integrated thermal and petrological model: *Lithos*, v. 149, p. 4–15. doi:10.1016/j.lithos.2012.01.010
- Hirth, G., Evans, R.L., and Chave, A.D., 2000, Comparison of continental and oceanic mantle electrical conductivity: Is the Archean lithosphere dry: *Geochemistry, Geophysics, Geosystems*, v. 1, p. 2000GC000048. doi:10.1029/2000GC000048
- Hirth, G., and Kohlstedt, D.L., 1996, Water in the oceanic upper mantle: Implications for rheology, melt extraction and the evolution of the lithosphere: *Earth and Planetary Science Letters*, v. 144, p. 93–108. doi:10.1016/0012-821X(96)00154-9
- Hoffman, P.F., and Schrag, D.P., 2002, The snowball Earth hypothesis: Testing the limits of global change: *Terra Nova*, v. 14, p. 129–155. doi:10.1046/j.1365-3121.2002.00408.x
- Jacobsen, S.B., 1988, Isotopic constraints on crustal growth and recycling: *Earth and Planetary Science Letters*, v. 90, p. 315–329. doi:10.1016/0012-821X(88)90133-1
- Jordan, T.H., 1978, Composition and development of the continental tectosphere: *Nature*, v. 274, p. 544–548. doi:10.1038/274544a0
- Jordan, T.H., 1988, Structure and formation of the continental tectosphere: *Journal of Petrology Special Volume*, p. 11–37. doi:10.1093/petrology/Special_Volume.1.11
- Kelly, R.K., Kelemen, P.B., and Jull, M., 2003, Buoyancy of the continental upper mantle: *Geochemistry, Geophysics, Geosystems*, v. 4, p. 1017. doi:10.1029/2002GC000399
- Knoll, A.H., and Carroll, S.B., 1999, Early animal evolution; emerging views from comparative biology and geology: *Science*, v. 284, p. 2129–2137. doi:10.1126/science.284.5423.2129
- Korenaga, J., Planavsky, N.J., and Evans, D.A.D., 2016, Global water cycle and the coevolution of the Earth's interior and surface environment: *Philosophical Transactions of the Royal Society A*, v. 375. doi:10.1098/rsta.2015.0393.
- Laske, G., Masters, G., Ma, Z., and Pasyanos, M., 2013, Update on CRUST1.0 - A 1-degree global model of Earth's crust: *Geophysica Researcher. Abstracts*, EGU2013-2658.
- Lee, C.-T.A., 2003, Compositional variation of density and seismic velocities in natural peridotites at STP conditions: Implications for seismic imaging of compositional heterogeneities in the upper mantle: *Journal of Geophysics Researcher*, v. 108. doi:10.1029/2003JB002413.
- Lee, C.-T.A., and Chin, E.J., 2014, Calculating melting temperatures and pressures of peridotite protoliths: Implications for the origin of cratonic mantle: *Earth and Planetary Science Letters*, v. 403, p. 273–286. doi:10.1016/j.epsl.2014.06.048
- Lee, C.-T.A., Lenardic, A., Cooper, C.M., Niu, F., and Levander, A., 2005, The role of chemical boundary layers in regulating the thickness of continental and oceanic thermal boundary layers: *Earth and Planetary Science Letters*, v. 230, p. 379–395. doi:10.1016/j.epsl.2004.11.019
- Lee, C.-T.A., Luffi, P., and Chin, E.J., 2011, Building and destroying continental mantle: *Annual Reviews Earth Planet Sciences*, v. 39, p. 59–90. doi:10.1146/annurev-earth-040610-133505
- Lee, C.-T.A., Luffi, P., Plank, T., Dalton, H.A., and Leeman, W.P., 2009, Constraints on the depths and temperatures of basaltic magma generation on Earth and other terrestrial planets using new thermobarometers for mafic magmas: *Earth and Planetary Science Letters*, v. 279, p. 20–33. doi:10.1016/j.epsl.2008.12.020
- Lee, C.-T.A., Shen, B., Slotnick, B.S., Liao, K., Dickens, G.R., Yokoyama, Y., Lenardic, A., Dasgupta, R., Jellinek, M., Lackey, J.S., Schneider, T., and Tice, M., 2013, Continental arc-island arc fluctuations, growth of crustal carbonates and long-term climate change: *Geosphere*, v. 9, p. 21–36. doi:10.1130/GES00822.1
- Lee, C.-T.A., Thurner, S., Paterson, S.R., and Cao, W., 2015, The rise and fall of continental arcs: Interplays between magmatism, uplift, weathering and climate: *Earth and Planetary Science Letters*, v. 425, p. 105–119. doi:10.1016/j.epsl.2015.05.045
- Lee, C.-T.A., Yeung, L.Y., McKenzie, N.R., Yokoyama, Y., Ozaki, K., and Lenardic, A., 2016, Two-step rise of atmospheric oxygen linked to the growth of continents: *Nature Geoscience*, v. 9, p. 417–424. doi:10.1038/ngeo2707
- Lenardic, A., and Moresi, L.-N., 1999, Some thoughts on the stability of cratonic lithosphere: Effects of buoyancy and viscosity: *Journal of Geophysical Research: Solid Earth*, v. 104, p. 12747–12758. doi:10.1029/1999JB900035
- Lyons, T.W., Anbar, A.D., Severmann, S., Scott, C., and Gill, B.C., 2009, Tracking euxinia in the ancient ocean: A multiproxy perspective and Proterozoic case study: *Annual Review of Earth and Planetary Sciences*, v. 37, p. 507–534. doi:10.1146/annurev.earth.36.031207.124233
- Lyons, T.W., Reinhard, C.T., and Planavsky, N.J., 2014, The rise of oxygen in Earth's early ocean and atmosphere: *Nature*, v. 506, p. 307–315. doi:10.1038/nature13068
- Maher, K., and Chamberlain, C.P., 2014, Hydrologic regulation of chemical weathering and the geologic carbon cycle: *Science*, v. 343, p. 1502–1504. doi:10.1126/science.1250770
- McGovern, P.J., and Schubert, G., 1989, Thermal evolution of the Earth: Effects of volatile exchange between atmosphere and interior: *Earth and Planetary Science Letters*, v. 96, p. 27–37. doi:10.1016/0012-821X(89)90121-0
- McKenzie, D., 1978, Some remarks on the development of sedimentary basins: *Earth and Planetary Science Letters*, v. 40, p. 25–32. doi:10.1016/0012-821X(78)90071-7
- McKenzie, D., and Priestley, K., 2016, Speculations on the formation of cratons and cratonic basins: *Earth and Planetary Science Letters*, v. 435, p. 94–104. doi:10.1016/j.epsl.2015.12.010
- Milliman, J.D., and Droessler, A.W., 1996, Neritic and pelagic carbonate sedimentation in the marine environment: Ignorance is not bliss: *Geological Rundschau*, v. 85, p. 496–504.
- Mills, B., Lenton, T.M., and Watson, A.J., 2014, Proterozoic oxygen rise linked to shifting balance between seafloor and terrestrial weathering: *Proceedings of the National Academy of Sciences*, v. 111, p. 9073–9078. doi:10.1073/pnas.1321679111
- Mooney, W.D., Laske, G., and Masters, G., 1998, CRUST 5.1: A global crustal model at: *Journal of Geophysical Research: Solid Earth*, v. 103, p. 727–747. doi:10.1029/97JB02122

- Ozaki, K., and Tajika, E., 2013, Biogeochemical effects of atmospheric oxygen concentration, phosphorus weathering, and sea-level stand on oceanic redox chemistry: Implications for greenhouse climates: *Earth and Planetary Science Letters*, v. 373, p. 129–139. doi:10.1016/j.epsl.2013.04.029
- Parsons, B., and McKenzie, D.P., 1978, Mantle convection and the thermal structure of the plates: *Journal of Geophysical Research*, v. 83, p. 4485–4495. doi:10.1029/JB083iB09p04485
- Parsons, B., and Sclater, J.G., 1977, An analysis of the variation of ocean floor bathymetry and heat flow with age: *Journal of Geophysical Research*, v. 82, p. 803–827. doi:10.1029/JB082i005p00803
- Pearson, D.G., Carlson, R.W., Shirey, S.B., Boyd, F.R., and Nixon, P.H., 1995, Stabilisation of Archaean lithospheric mantle: A Re-Os isotope study of peridotite xenoliths from the Kaapvaal craton: *Earth and Planetary Science Letters*, v. 134, p. 341–357. doi:10.1016/0012-821X(95)00125-V
- Pearson, D.G., and Wittig, N., 2008, Formation of Archaean continental lithosphere and its diamonds: The root of the problem: *Journal of the Geological Society*, v. 165, p. 895–914. doi:10.1144/0016-76492008-003
- Peters, S.E., and Gaines, R.R., 2012, Formation of the ‘Great Unconformity’ as a trigger for the Cambrian explosion: *Nature*, v. 484, p. 363–366. doi:10.1038/nature10969
- Phillips, R.J., and Lambeck, K., 1980, Gravity fields of the terrestrial planets: Long wavelength anomalies and tectonics: *Reviews of Geophysics*, v. 18, p. 27–76. doi:10.1029/RG018i001p00027
- Pierrehumbert, R.T., 2010, *Principles of planetary climate*: Cambridge, Cambridge University Press.
- Pollack, H.N., 1986, Cratonization and thermal evolution of the mantle: *Earth and Planetary Science Letters*, v. 80, p. 175–182. doi:10.1016/0012-821X(86)90031-2
- Prokoph, A., Shields, G.A., and Veizer, J., 2008, Compilation and time-series analysis of a marine carbonate $d^{18}O$, $d^{13}C$, $87Sr/86Sr$ and $d^{34}S$ database through Earth history: *Earth-Science Reviews*, v. 87, p. 113–133. doi:10.1016/j.earscirev.2007.12.003
- Pufahl, P.K., and Hiatt, E.E., 2012, Oxygenation of the Earth’s atmosphere—ocean system: A review of physical and chemical sedimentologic responses: *Marine and Petroleum Geology*, v. 32, p. 1–20. doi:10.1016/j.marpetgeo.2011.12.002
- Putirka, K.D., 2005, Mantle potential temperatures at Hawaii, Iceland, and the mid-ocean ridge system, as inferred from olivine phenocrysts: Evidence for thermally driven mantle plumes: *Geochemistry, Geophysics, Geosystems*, v. 6. doi:10.1029/2005GC000915
- Reinhard, C.T., Planavsky, N.J., Gill, B., Ozaki, K., Robbins, L.J., Lyons, T.W., Fischer, W.W., Wang, C., Cole, D.B., and Konhauser, K.O., 2017, Evolution of the global phosphorus cycle: *Nature*, v. 541, p. 386–389. doi:10.1038/nature20772
- Ridgwell, A., 2005, A Mid-Mesozoic revolution in the regulation of ocean chemistry: *Marine Geology*, v. 217, p. 339–357. doi:10.1016/j.margeo.2004.10.036
- Ridgwell, A., and Zeebe, R.E., 2005, The role of the global carbonate cycle in the regulation and evolution of the Earth system: *Earth and Planetary Science Letters*, v. 234, p. 299–315. doi:10.1016/j.epsl.2005.03.006
- Rozanski, K., Araguas-Araguas, L., and Gonfiantini, R., 1993, Isotopic patterns in modern global precipitation, in Swart, P.K., Lohmann, K.C., McKenzie, J.A., and Svin, S.M., eds., *Climate change in continental isotopic records: American Geophysical Union Monograph*, v. 78, p. 1–36.
- Ruttenberg, K.C., 2003, *The global phosphorous cycle: Treatise of Geochemistry*, v. 8, p. 585–643.
- Sagan, C., and Mullen, G., 1972, Earth and Mars: Evolution of atmospheres and surface temperatures: *Science*, v. 177, p. 52–56. doi:10.1126/science.177.4043.52
- Sandu, C., Lenardic, A., and McGovern, P., 2011, The effects of deep water cycling on planetary thermal evolution: *Journal of Geophysical Research: Solid Earth*, v. 116. doi:10.1029/2011JB008405
- Schiffbauer, J.D., Huntley, J.W., O’Neil, G.R., Darroch, S.A.F., Laflamme, M., and Cai, Y., 2016, The latest Ediacaran wormworld fauna: Setting the ecological stage for the Cambrian explosion: *Geological Society of America Today*, v. 26, p. 4–11.
- Simoes, M., Braun, J., and Bonnet, S., 2010, Continental-scale erosion and transport laws: A new approach to quantitatively investigate macroscale landscapes and associated sediment fluxes over the geological past: *Geochemistry Geophysics Geosystems*, v. 11, p. Q09001. doi:10.1029/2010GC003121
- Sloss, L.L., 1963, Sequences in the cratonic interior of North America: *Geological Society of America Bulletin*, v. 74, p. 93–114. doi:10.1130/0016-7606(1963)74[93:SITCIO]2.0.CO;2
- Vlaar, N.J., 2000, Continental emergence and growth on a cooling earth: *Tectonophysics*, v. 322, p. 191–202. doi:10.1016/S0040-1951(00)00063-9
- Volk, T., 1989, Rise of angiosperms as a factor in long-term climatic cooling: *Geology*, v. 17, p. 107–110. doi:10.1130/0091-7613(1989)017<0107:ROAAAF>2.3.CO;2
- Walker, L.J., Wilkinson, B.H., and Ivany, L.C., 2002, Continental drift and Phanerozoic carbonate accumulation in shallow-shelf and deep-marine settings: *The Journal of Geology*, v. 110, p. 75–87. doi:10.1086/324318
- Wieczorek, M.A., 2007, Gravity and topography of the terrestrial planets: *Treatise of Geophysics*, v. 10, p. 165–206.
- Winnick, M.J., Chamberlain, C.P., Caves, J.K., and Welker, J.M., 2014, Quantifying the isotopic ‘continental effect’: *Earth and Planetary Science Letters*, v. 406, p. 123–133. doi:10.1016/j.epsl.2014.09.005
- Young, G.M., Von Brunn, V., Gold, D.J.C., and Minter, W.E.L., 1998, Earth’s oldest reported glaciation: Physical and chemical evidence from the archaean mozaan Group (2.9 Ga) of South Africa: *The Journal of Geology*, v. 106, p. 523–538. doi:10.1086/516039

Appendix

Isostatic equations

Elevations are calculated assuming isostasy, where the compensation depth is below the lithospheric mantle root. For the case in which continents ride above sea level, the elevation of continents above sea level h_e can be determined using the following isostatic balance (see Table 1):

$$\rho_{cc}h_{cc} + \rho_{cr}h_{cr} = \rho_w h_{ow} + \rho_{oc}h_{oc} + \rho_{or}h_{or} + \rho_a(h_{cc} + h_{cr} - h_{oc} - h_{or} - h_e - h_{ow}), \quad (1)$$

where ρ_w , ρ_{cc} , ρ_{cr} , ρ_{oc} , ρ_{or} , and ρ_a are the densities of sea water, continental crust, continental lithospheric mantle root, oceanic crust, oceanic lithospheric mantle root, and asthenospheric mantle, h_{ow} is the average depth of the ocean, and h_{cc} , h_{cr} , h_{oc} , and h_{or} are the thicknesses of the continental crust, continental lithospheric mantle root, oceanic crust and oceanic lithospheric mantle root. When continents are submerged, the depth of continents below sea level h_{cw} is given by the following isostatic balance:

$$\rho_{cc}h_{cc} + \rho_w h_{cw} + \rho_{cr}h_{cr} = \rho_w h_{ow} + \rho_{oc}h_{oc} + \rho_{or}h_{or} + \rho_a(h_{cc} + h_{cr} + h_{cw} - h_{oc} - h_{or} - h_{ow}). \quad (2)$$

For a given volume of ocean water, V_w , the mass balance relationship between the amount of water in ocean basins and above submerged continents is given by

$$h_{ow}A_{oc} + h_{cw}A_{cc} = V_w, \quad (3)$$

where A_{oc} is the area of ocean basins, A_{cc} is the area of continents and $A_{oc} + A_{cc}$ is the surface area of the Earth. If total water volume has remained constant through time, then V_w is the product of today's average ocean depth h_{ow}^* and the area of oceanic basins A_{oc}^* , that is, $V_w = h_{ow}^*A_{oc}^*$.

Densities of each layer are referenced relative to the temperature of the ambient convecting mantle, which we take to be the mantle potential temperature T_m . Thus, relative change in density due to temperature differences between a given layer i are given by

$$\frac{\rho_i}{\rho_i^0} = 1 + \alpha(T_m - T_i), \quad (4)$$

where T_i represents the average temperature of layer i , ρ_i^0 is the material density at standard temperature and pressure conditions, and α is thermal expansivity. Assuming the temperature of the surface is zero, temperature at the base of the lithosphere is T_m , and the geotherm is roughly linear, average temperatures for each layer are given by

$$T_{oc} = \frac{h_{oc}T_m}{2(h_{oc} + h_{or})}, \quad (5a)$$

$$T_{or} = \frac{(h_{oc} + h_{or}/2)T_m}{h_{oc} + h_{or}}, \quad (5b)$$

$$T_{cc} = \frac{h_{cc}T_m}{2(h_{cc} + h_{cr})}, \quad (5c)$$

$$T_{cr} = \frac{(h_{cc} + h_{cr}/2)T_m}{h_{cc} + h_{cr}}. \quad (5d)$$

When modelling how elevations change with time, we must model how crustal and lithospheric mantle root thickness

change. We assume that since ~ 2.5 Ga, mantle convection has operated in a mobile lid regime. We assume that the oceanic crust is formed by mid-ocean ridge spreading, such that the thickness of the crust is controlled to first order by mantle potential temperature. We use the following parameterization for oceanic crust thickness (Galer and Mezger, 1998):

$$h_{oc} = 0.00015T_m^2 - 0.345T_m + 200. \quad (6)$$

We assume that the oceanic lithospheric mantle root thickness h_{or} is equal to the characteristic thermal boundary layer thickness of the convecting system, which assumes that the boundary layer grows by conductive cooling. That is,

$$h_{or} = \sqrt{4\kappa\tau_{oc}}, \quad (7)$$

where κ is thermal diffusivity and τ_{oc} is the lifespan of oceanic crust. The average lifespan of oceanic crust is approximated by

$$\tau_{oc} = \tau^*u^*/u, \quad (8)$$

where τ^* is the modern lifespan of oceanic crust, u^* is the average modern plate velocity and u is the average plate velocity at the time of interest. This relationship assumes that the area of ocean basins has remained approximately constant, not an unreasonable assumption given that most of the continents are thought to have formed by 2 Ga.

To calculate average plate velocities, we again assume a mobile-lid regime. Assuming also that the convecting system is at statistical steady state, we can use parametrized convection models. Thus, the average plate velocity for a given mantle potential temperature T_m , relative to the present day state, is given by Flament et al., (2008):

$$\frac{u}{u^*} = \left(\frac{T_m\eta^*}{T_m^*\eta} \right)^n, \quad (9)$$

where T_m^* is modern mantle potential temperature, η^* is present day average mantle viscosity, η is the mantle viscosity at the time of interest, and n is an exponent describing the nature of convection. A maximum bound is 0.66 and corresponds to a bottom-heated system with weak plates. An internally heated system would have a value of ~ 0.5 , with strong plates decreasing n further. We thus considered n between 0.2 and 0.66. Viscosity relative to present day is given by

$$\frac{\eta}{\eta^*} = \exp\left(\frac{E}{RT} - \frac{E}{RT_m^*}\right), \quad (10)$$

where E is the activation energy and R is the gas constant. We assumed an activation energy of 350 kJ/mol.

Thickness of the continental crust and continental lithospheric mantle root are also dynamic quantities. Continental crustal thickness is controlled by processes that thin and thicken the crust. Thinning is controlled by erosion, extensional tectonics or gravitational collapse of the lower crust. Thickening is driven by magmatism or compressional tectonics. The following equation describes the evolution of crustal thickness:

$$\frac{dh_{cc}}{dt} = \dot{M} - \dot{E}, \quad (11)$$

where M is the thickening forcing function and E represents thinning (Lee et al., 2015). We assume that thinning is primarily controlled by erosion, which we assume scales with average elevation (Simoes et al., 2010):

$$\dot{E} = k_e h_e, \quad (12)$$

where k_e is an erosion rate constant, whose inverse represents the average response time (or e-fold decay time) of a mountain undergoing erosion. Continental elevation h_e is controlled by isostasy, following Equations (1) and (2). If continental elevations are below sea level, the second term in Equation (11) should be positive and k_e becomes a rate constant characteristic of sedimentation. It is important to note that k_e need not be constant; it can be varied as a function of time or continental elevation. Continental lithospheric mantle root thickness h_{cr} evolves with time t following conductive cooling:

$$h_{cr} = \sqrt{4kt}. \quad (13)$$

Root growth is terminated when the thickness approaches that of the chemical boundary layer.

Element distribution in ocean

A simple model was developed for tracking the distribution of elements, which are sensitive to redox or have a strong affinity for organic carbon. We assume that the system is at steady, such that total inputs J_{in} of an element (moles/year) is balanced by the total output, which we take to be the sum of outputs in oxic environments J_{ox} and anoxic or suboxic environments J_{an} :

$$J_{in} = J_{an} + J_{ox}. \quad (14)$$

On continental margins, the combination of nutrient upwelling and shallower depths allow the oxygen minimum zone to more closely approach the sediment water interface in continental margins than in open ocean environments. Although clearly an approximation, we thus equate sedimentation in the open ocean to be oxic and along continental margins to be anoxic or suboxic. Equation (14) can be expressed in terms of the output flux (moles/m²/year) for open ocean j_{ox} and continental margins j_{an} :

$$J_{in} = j_{an} f_{an} A_{cc} + j_{ox} A_{oc}, \quad (15)$$

where A_{cc} and A_{oc} are the areas of continental crust and oceanic crust and f_{an} represents the fraction of continents that lie below sea level, e.g. the fraction of continental margins relative to continental area. We can then define effective seawater partition coefficients D for anoxic/suboxic and oxic sediments:

$$D_{an} = j_{an} / C_{ow}, \quad (16a)$$

$$D_{ox} = j_{ox} / C_{ow}, \quad (16b)$$

where C_{ow} is the total mass (moles) of the element of interest in seawater, assuming a well-mixed ocean. The units of the effective partition coefficient are m⁻²year⁻¹ and therefore

represents the probability that the element of interest in seawater will be sequestered in a square metre of sediment per year. Thus, the partition coefficient represents an effective rate constant for burial. The effective partition coefficient is an attempt to encapsulate in a single number what is otherwise a very complex process, where element output rate depends on such factors as sedimentation rate, organic carbon delivery, metal chelation, etc. Given that all of these factors can vary considerably, we assume that the effective partition coefficient globally averages out these variations.

Because we are not able to directly measure globally averaged partition coefficients, we have to estimate these values. Equations (15) and (16) can be re-expressed to estimate a present day (*) partition coefficient for anoxic/suboxic and oxic sediments:

$$D_{an} = \left(\frac{J_{an}^*}{J_{in}^*} \right) \frac{J_{in}^*}{f_{an}^* A_{cc}^* C_{ow}^*}, \quad (17a)$$

$$D_{ox} = \left(\frac{J_{ox}^*}{J_{in}^*} \right) \frac{J_{in}^*}{A_{oc}^* C_{ow}^*}. \quad (17b)$$

Here, the quantities in parentheses J_{an}^*/J_{in}^* and J_{ox}^*/J_{in}^* represent the fraction that gets deposited in anoxic/suboxic and oxic sediments, quantities that can be constrained based on mass balance studies in marine sediments. In our models, we explore the sensitivity to these fractional burial estimates. Assuming that these effective partition coefficients are constant for a given environment, anoxic/suboxic and oxic, we can combine the above equations and re-arrange to arrive at an expression of the concentration of the element of interest in seawater relative to the present day:

$$\frac{C_{ow}}{C_{ow}^*} = \left(\frac{J_{in}}{J_{in}^*} \right) \frac{D_{an} f_{an}^* X_{cc}^* + D_{ox} (1 - X_{cc}^*)}{D_{an} f_{an} X_{cc} + D_{ox} (1 - X_{cc})}, \quad (18)$$

where X_{cc} represents the fraction of continental area relative to the surface area of the Earth (A_{cc}/A_{Earth}). Equation (18) shows that the concentration of an element in seawater depends on the area of submerged continents and ocean basins as well as the inputs.

To calculate what fraction of continents are submerged, we assume an exponential shape of continents

$$y = (h_{ow} + h_e)(1 - \exp(-f/b)), \quad (19)$$

where y is the elevation above the seafloor, f is the areal fraction of crust relative to the total continental surface area ($0 < f < 1$), and b is a constant representing some measure of how wide continental margins are. That is, Equation (19) describes a plateau-like continental profile with steep shoulders of approximate width b . How much of the shoulder is submerged f_{an} is determined by letting $y = h_{ow}$ in Equation (19) and rearranging to yield

$$f_{an} = -b \ln \left(1 - \frac{h_{ow}}{h_{ow} + h_e} \right). \quad (20)$$